

## SUPPORTING INFORMATION

# Unexpected Enzyme-Catalyzed Regioselective Acylation of Flavonoid Aglycones

Eleni Kyriakou<sup>1</sup>, Alexandra Primikyri<sup>1</sup>, Pantelis Charisiadis<sup>1</sup>, Maria Katsoura<sup>2</sup>, Ioannis P. Gerothanassis<sup>1</sup>, Haralambos Stamatis<sup>2</sup>, Andreas G. Tzakos<sup>1</sup>

<sup>1</sup>Department of Chemistry, Section of Organic Chemistry and Biochemistry, 45110, Ioannina, Greece, <sup>2</sup>Laboratory of Biotechnology, Department of Biological Applications and Technologies, University of Ioannina, 45110 Ioannina, Greece

### Corresponding Author

\*Tel: +30 2651 00 8387. E-mail: [atzakos@cc.uoi.gr](mailto:atzakos@cc.uoi.gr)

### Table of contents

1. Materials and methods	2
2. HPLC & MS	2
3. Nuclear Magnetic Resonance (NMR)	3
4. Docking calculations	3
5. HPLC chromatogram of the blank and the enzymatic reaction products of quercetin ( <b>Figure S1</b> )	4
6. <b>Figure S2</b>	5
5. <b>Figure S3</b>	6
6. 1D <sup>1</sup> H NMR spectrum of quercetin ( <b>Figure S4</b> )	7
7. 2D <sup>1</sup> H- <sup>13</sup> C HSQC NMR spectrum of quercetin ( <b>Figure S5</b> )	8
8. 2D <sup>1</sup> H- <sup>13</sup> C HMBC NMR spectrum of quercetin ( <b>Figure S6</b> )	9
9. MS spectrum of the enzymatic reaction products of quercetin ( <b>Figure S7</b> )	10
10. MS spectrum of the enzymatic reaction products of naringenin ( <b>Figure S8</b> )	11
11. 1D <sup>1</sup> H NMR spectrum of quercetin and its analogues (Q1 and Q2) ( <b>Figure S9</b> )	12
12. 2D <sup>1</sup> H- <sup>13</sup> C HSQC NMR spectrum of quercetin derivatives Q1 and Q2 ( <b>Figure S10</b> )	13
13. 2D <sup>1</sup> H- <sup>13</sup> C HMBC NMR spectrum of quercetin derivatives Q1 and Q2 ( <b>Figure S11</b> )	14
14. Protocols used to assign the molecule. Selected regions from 500 MHz 2D <sup>1</sup> H- <sup>13</sup> C HSQC, 2D <sup>1</sup> H- <sup>13</sup> C HMBC NMR spectrum of the acylated derivatives of quercetin <b>Figure S12</b> , <b>Figure S13</b> and <b>Figure S14</b>	15-17
15. 1D <sup>1</sup> H NMR spectrum of naringenin (N) and its analogue (N1) ( <b>Figure S15</b> )	18
16. 1D <sup>1</sup> H NMR spectrum of hyperoside (H) and its analogue (H1) before and after the addition of picric acid ( <b>Figure S16</b> )	19
17. 1D <sup>1</sup> H NMR spectrum of hyperoside (H) and its analogue (H1) before and after the addition of picric acid peak of water ( <b>Figure S17</b> )	20
18. Full <sup>1</sup> H and <sup>13</sup> C chemical shift assignments of quercetin ( <b>Table S1</b> )	21
19. Full <sup>1</sup> H and <sup>13</sup> C chemical shift assignments of the 3'-acetyl derivative of quercetin (Q1) ( <b>Table S2</b> )	22
20. Full <sup>1</sup> H and <sup>13</sup> C chemical shift assignments of the 4'-acetyl derivative of quercetin (Q2) ( <b>Table S3</b> )	23
21. Full <sup>1</sup> H and <sup>13</sup> C chemical shift assignments of naringenin ( <b>Table S4</b> )	24
22. Full <sup>1</sup> H and <sup>13</sup> C chemical shift assignments of the 4'-acetyl derivative of naringenin (N1) ( <b>Table S5</b> )	25

## 1. Materials and methods

### 1.1 Reagents

*Candida antarctica* lipase B (Novozym 435<sup>®</sup>) immobilized on acrylic resin, obtained from Novo Nordisk A/S. Flavonoids aglycons (Quercetin and naringenin anhydrous), glycosylated flavonoid (hyperoside), organic solvents (2-methyl-2-butanol and CH<sub>3</sub>CN) and vinyl esters (Vinyl acetate and Vinyl butyrate) were purchased from Sigma and were of the highest available purity.

### 1.2 Enzymatic Reactions

Each reaction was prepared by dissolving 1 mg of each flavonoid (3 μmol) and glycosylated flavonoid (2 μmol) in 200 μl of solvent (CH<sub>3</sub>CN, 2-methyl-2-butanol or acetone), adding 12 mg Novozyme 435 (60 mg/ml) and 1 mmol (100 μl) of acyl donor (vinyl acetate or vinyl butyrate). The enzymatic acylation of flavonoids in organic solvents (CH<sub>3</sub>CN, 2-methyl-2-butanol and acetone) was carried out in stirred flasks that were incubated in an orbital shaker at 250 rpm at 50° C for acetone and 60° C for the other solvents). For the acylation vinyl esters were used as acylation reagents, since they are poor nucleophiles, a fact that makes the acylation reaction virtually irreversible during the transesterification, also during the reaction acetaldehyde is produced as byproduct that is volatile and thus is eliminated. The reactions were initially performed for 168 hrs (7 days) in the aforementioned three solvents. The reaction mixture in each case was filtered using a Nylaflo<sup>™</sup> Nylon membrane filter particle size 0.45 μm and diameter 13mm. The substrates and products of the biocatalytic reaction were monitored by HPLC. The reaction products were characterized by MS and multidimensional NMR experiments. For the specific reaction time (7 days) the best yield was obtained for acetone (71.2 % as compared to 67.9 % for CH<sub>3</sub>CN and 39.2 % for 2-methyl-2-butanol, Fig. S2). The reactions were repeated for 72 hrs and again acetone provided the best yield (45%). Constructively, the optimum reaction conditions were as follows: time 72 hrs, vinyl acetate as the acyl donor, acetone as the solvent. The isolated yield for the quercetin monoacylation products was 0.46 mg, 1.40 μmol, 45% yield. Following the same optimum reaction conditions for naringenin resulted in 0.71 mg, 2.30 μmol, 71% yield as for naringenin monoacylation products. As for the hyperoside the product yield was 97%, 1.90 μmol, 1.08 mg.

## 2. HPLC & MS

Quantitative analysis of Quercetin and its ester derivative was performed by HPLC, using a  $\mu$ Bondapak C18 column, particle size 10 $\mu$ m, length 300 mm, diameter 3.9mm and a diode array UV detector. The mobile phase was 90:10 (v/v) H<sub>2</sub>O/CH<sub>3</sub>CN (in 0.1% of acetic acid). A gradient from this mobile phase (0:100 (v/v) H<sub>2</sub>O/CH<sub>3</sub>CN) was performed in 25 min, and this eluent was maintained during 5 min. This linear gradient was employed for 30 min. The elution was performed at 27° C, with a flow rate of 1 mL/min. Purified flavonoid esters were obtained by semi-preparative HPLC. A C18 column with particle size 10  $\mu$ m, length 250 mm, diameter 21.2 mm was used. Linear gradient from 10 to 100% acetonitrile in water (containing 0.1% acetic acid) was employed for 30 min. The elution was performed at 27° C at a flow rate of 2 ml/min. All LC-MS experiments were performed on a quadrupole ion trap mass analyzer (Agilent Technologies, model MSD trap SL) retrofitted to a 1100 binary HPLC system equipped with an degasser, autosampler, diode array detector and electrospray ionization source (Agilent Technologies, Karlsruhe, Germany). All hardware components were controlled by Agilent Chemstation Software.

## 3. Nuclear Magnetic Resonance (NMR).

As pointed above the reaction took place in no aqueous media to avoid enzymatic hydrolysis in the presence of water. Directly after the reaction the immobilized enzyme was removed by filtration the solvent was evaporated and the crude reaction products were dissolved in 400  $\mu$ l of DMSO-d<sub>6</sub>. In order to enhance the spectral quality, especially for the OH region, each sample was titrated with a small amount of picric acid from a stock solution of 10.18 mM (18  $\mu$ mol) in DMSO-d<sub>6</sub>. In each sample 2-5  $\mu$ l of the stock solution was added. For instance, in case of the reaction of quercetin 25.30 nmol of picric acid (2.5  $\mu$ l) were added (molar ratio of picric acid and flavonoid was 1:53) and as for the reaction of hyperoside 44.50 nmol of picric acid (4.5  $\mu$ l) was added (molar ratio of picric acid and flavonoid was 1:44). All NMR experiments were conducted on a Bruker avance 500MHz AV spectrometer equipped with a cryoprobe. The pulse sequences for <sup>1</sup>H-<sup>13</sup>C HSQC, <sup>1</sup>H-<sup>13</sup>C HMBC were standard Bruker library sequences, acquired with 2 K data points over a 14 ppm spectral width. DOSY experiments were performed using the bipolar longitudinal eddy current delay (BPPLIED) pulse sequence, with the following gradient

parameters: p19 (gradient length) 1.1ms, d1 (relaxation delay) 5s, p1 (90o pulse) 8.15 $\mu$ s and d16 (delay for gradient recovery) 200  $\mu$ s and d21 (eddy current delay) 5ms. The diffusion time  $\Delta$  was adjusted to 50 ms and the gradient duration was optimized in order to obtain 7% residual signal with the maximum gradient strength resulting in a  $\delta$  value of 5600 $\mu$ s. The gradient strength was incremented from 5 to 95% of its maximum in a linear ramp. In each PFG NMR experiment, a series of 16 BPPLIED spectra were acquired at 298K and 16K data points were collected. The diffusion dimension was zero-filled to 32. The diffusion dimension was exponentially fitted according to a preset window with log D from -12.0 to -8.0.

#### ***4. Docking calculations***

The CALB crystal structure was obtained from the Protein Data Bank (PDB entry: 1LBS; resolution: 2.60 Å). Flexible docking calculations were performed treating H224 and Ser105 as flexible residues with autodock vina (Trott, O.; Olson, A. J. *J Comput Chem* **2011**, *31*, 455-61) and leadit (<http://www.biosolveit.de/>). Standard docking protocols were used (see Tzakos et al. *Chembiochem*. 2005 Jun;6(6):1089-103.).

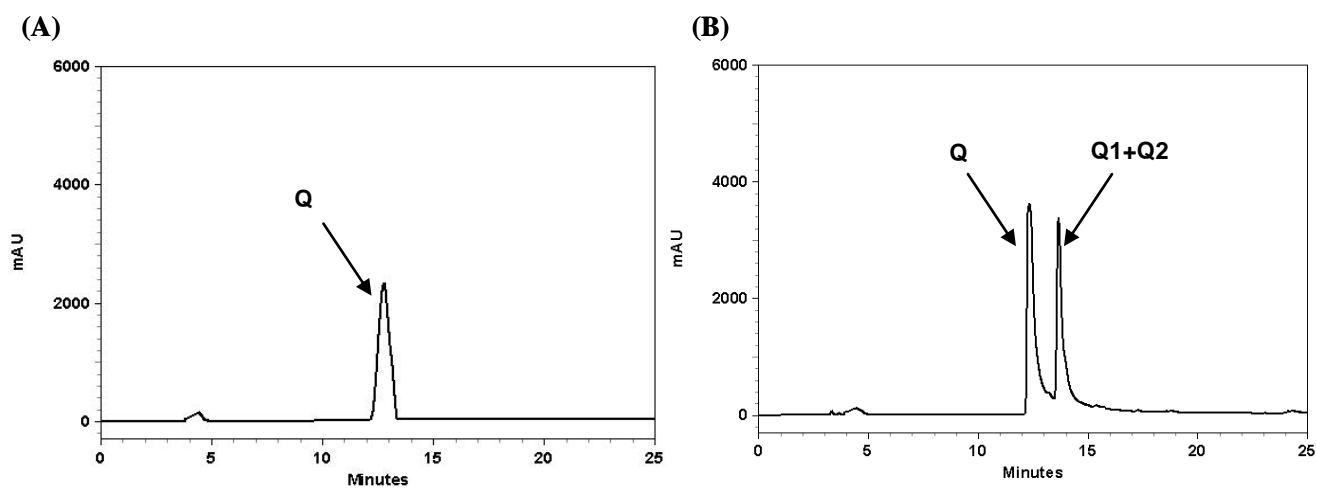


**Figure S1.** (A) HPLC chromatogram of the quercetin (blank). The fraction at  $t_R = 12.5$  min belong to quercetin. (B) HPLC chromatogram of the enzymatic reaction. The first fraction ( $t_R = 12.5$  min) belongs to unreacted quercetin and the second ( $t_R = 14.3$  min) corresponds to the monoacylated products (Q1, Q2).

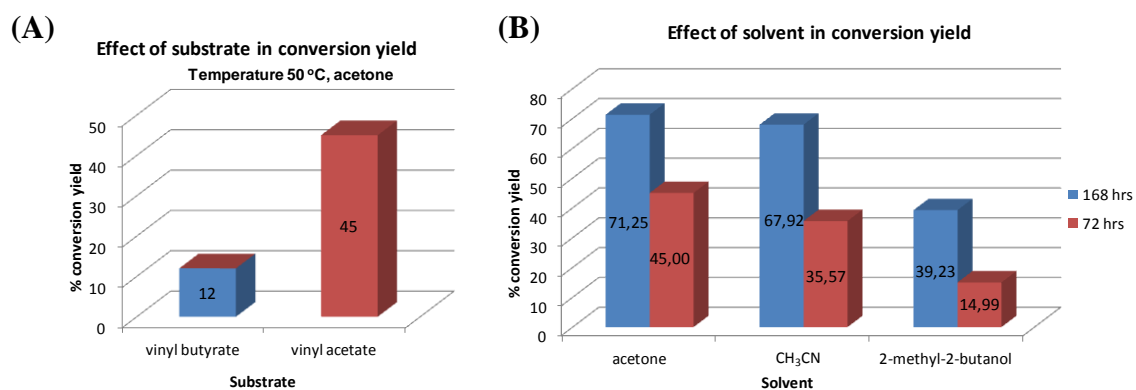


**Figure S2.** Effects of substrate (A) (1: vinyl butyrate and 2: vinyl acetate) and (B) solvent in the acylation conversion yield of quercetin by CALB (Novozym 435) for 72 hrs and 168 hrs colored in red and blue, respectively.

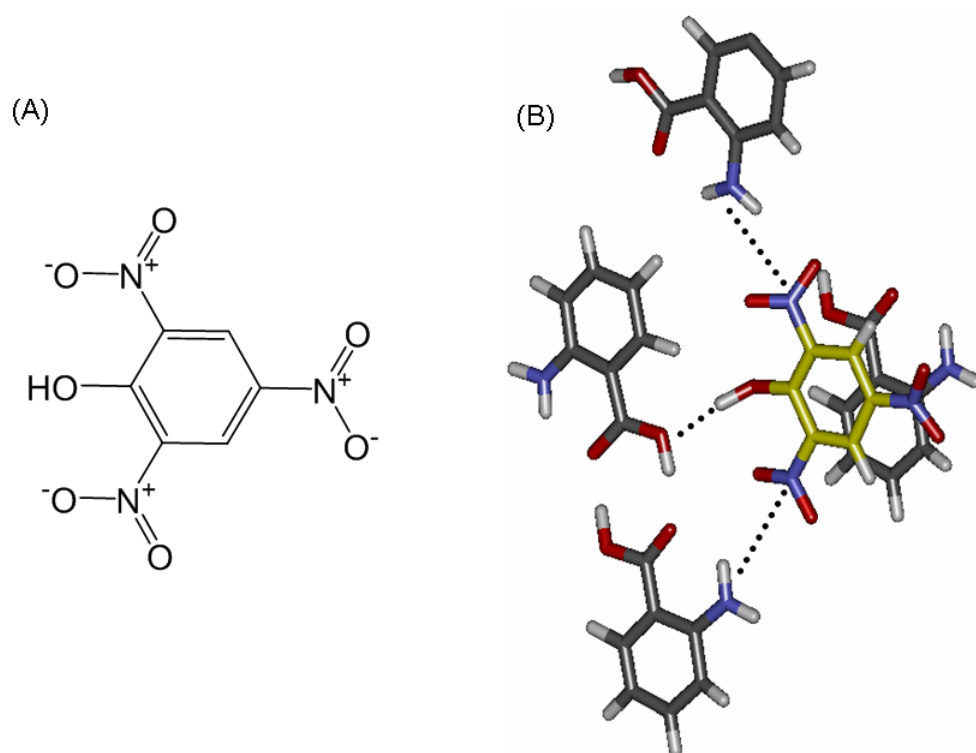


**Figure S3.** (A) Picric acid can be employed in numerous interactions such as electrostatic, hydrogen bonding, and  $\pi$ - $\pi$  stacking. (B) An example of these interactions between a single picric acid molecule (carbon skeleton colored in yellow) and four anthranilic acid molecules (carbon skeleton colored in grey) is illustrated. Dashed lines indicate hydrogen bonding interactions between anthranilic acid and the polar nitro and phenol O atoms of picric acid (Y In et al., *Acta Cryst.* (1997). C53, 646-648).

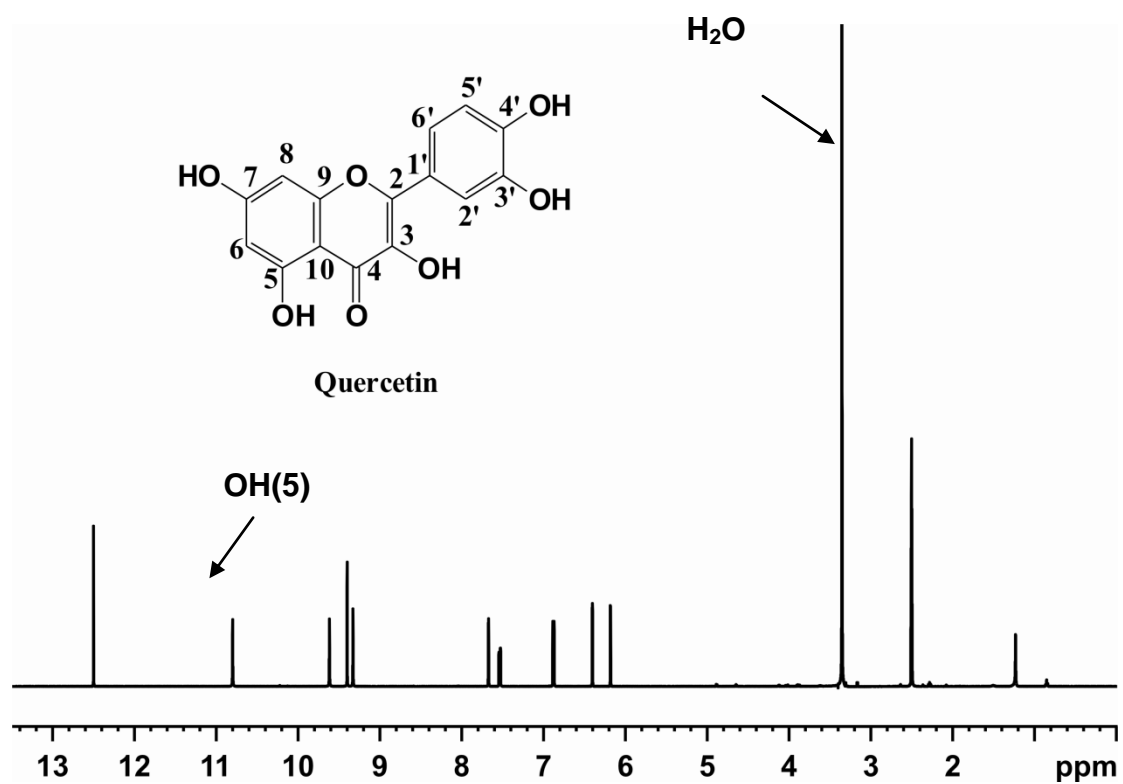


**Figure S4.** 1D <sup>1</sup>H NMR spectrum of quercetin in 500 μl DMSO-d<sub>6</sub> (T= 298 K, number of scans = 5). The 2D structure of quercetin is shown as inset.

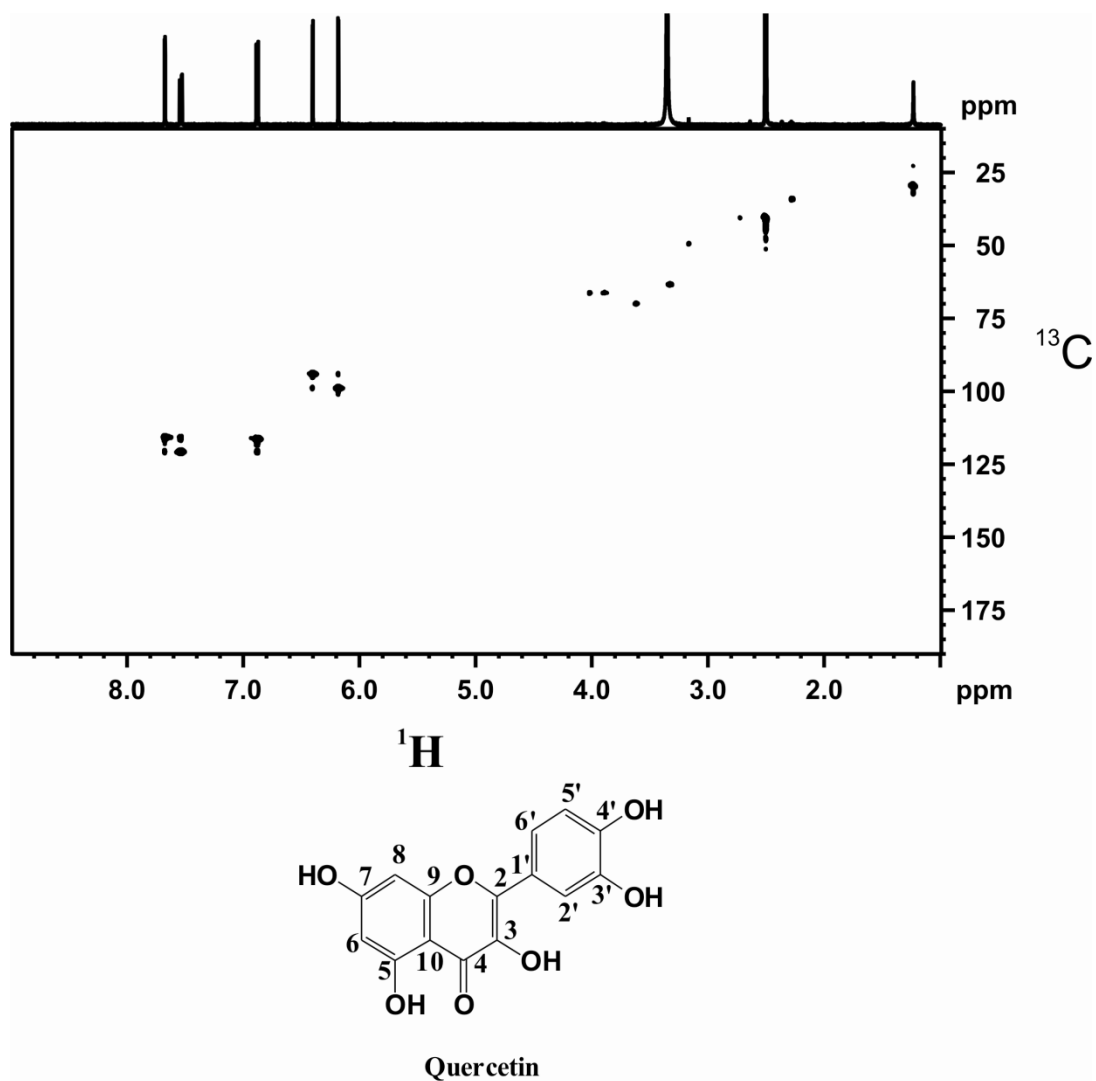


**Figure S5.** 500 MHz 2D  $^1\text{H}$ - $^{13}\text{C}$  HSQC NMR spectrum of quercetin in 500  $\mu\text{l}$   $\text{DMSO-d}_6$  ( $T=298\text{ K}$ , number of scans = 8). The 2D structure of quercetin is shown below.

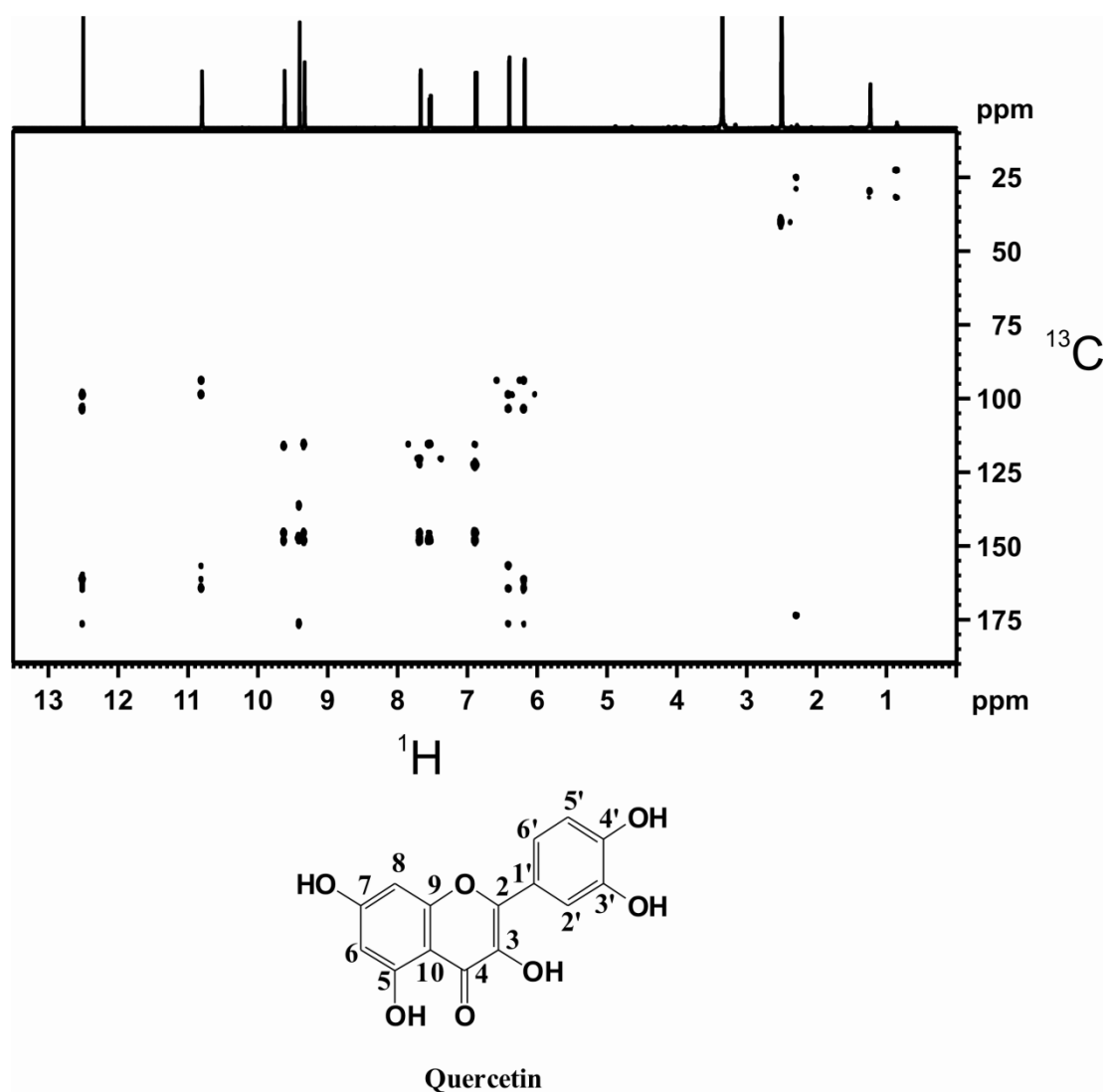


**Figure S6.** 500 MHz 2D  $^1\text{H}$ - $^{13}\text{C}$  HMBC NMR spectrum of quercetin in 500  $\mu\text{l}$  DMSO- $d_6$  ( $T=298\text{ K}$ , number of scans = 36). The 2D structure of quercetin is shown below.

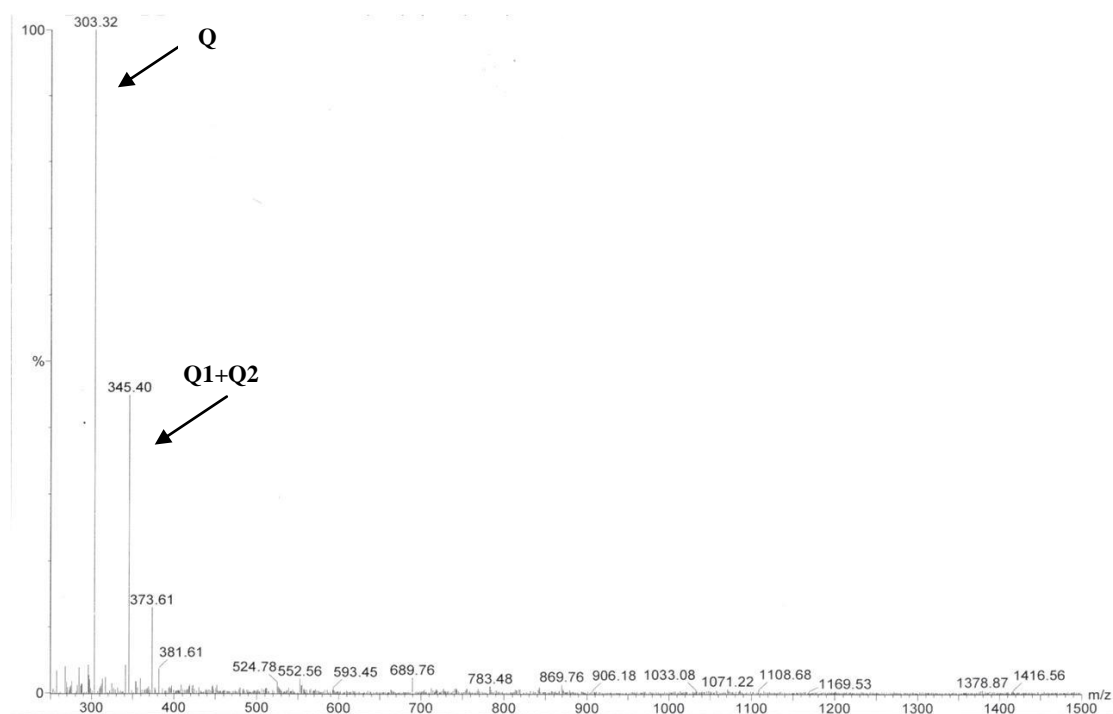


**Figure S7.** MS spectrum of the reaction products of quercetin indicates that monoacylation took place. The first peak at  $m/z=303.32$  is the molecular weight of unreacted quercetin, Q (302.24) and the second peak at  $m/z=345.40$  corresponds to the molecular weight of the monoacetyl ester of quercetin (Q1, Q2).

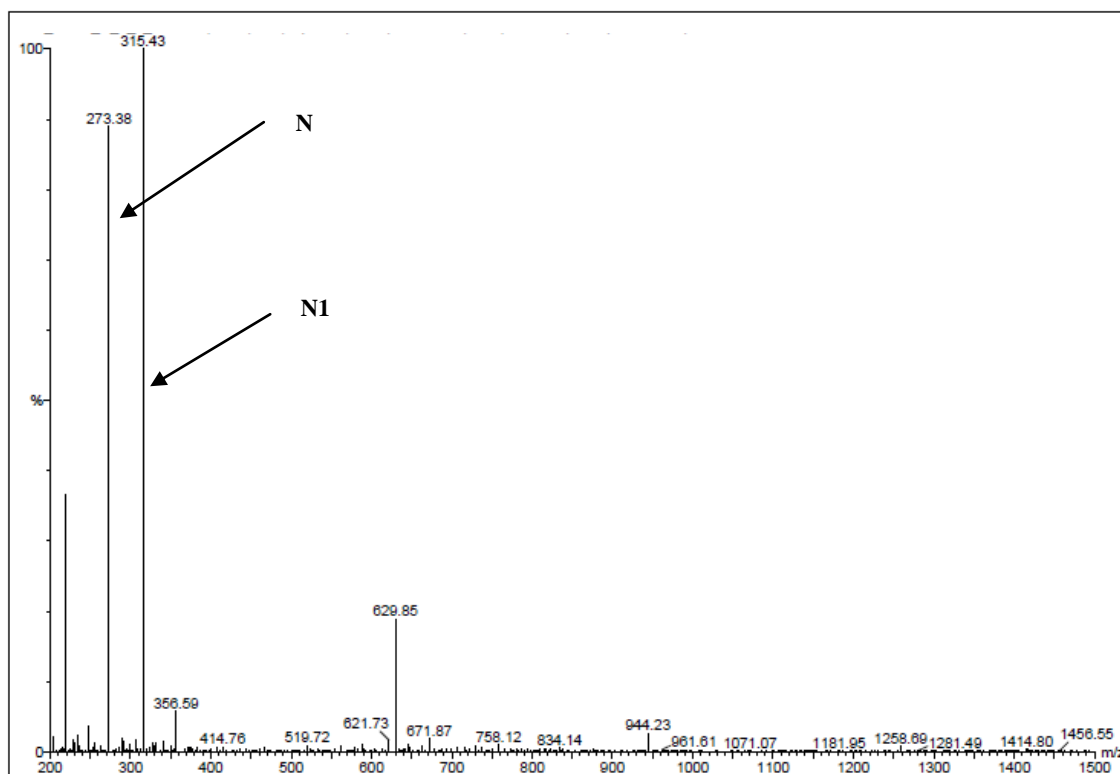


**Figure S8.** MS spectrum of the reaction products of naringenin indicates that monoacylation took place. The first peak at  $m/z=273.38$  is the molecular weight of unreacted naringenin, N (272.25) and the second peak at  $m/z=315.43$  corresponds to the molecular weight of the monoacetyl ester of naringenin (N1).

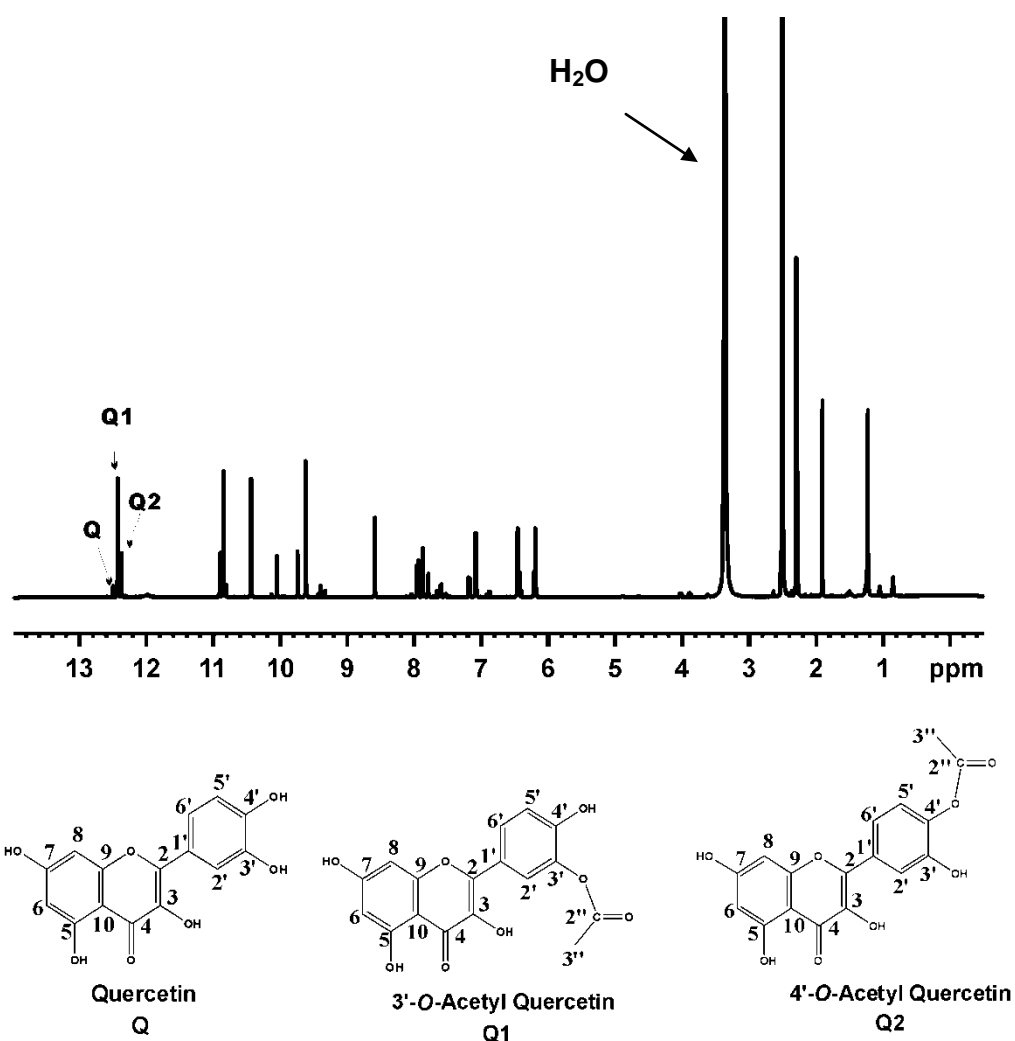


**Figure S9.** 1D <sup>1</sup>H NMR spectrum of quercetin (Q) and its analogues (Q1 and Q2) in 500 μl DMSO-d<sub>6</sub> (T= 298 K, number of scans = 256). The three strongly deshielded resonances above 12.5 ppm correspond to the OH(5) protons of Q, Q1 and Q2 (shown in the spectrum with arrows) participating in intramolecular hydrogen bonding with the carbonyl group CO(4). The 2D structures of quercetin and its derivatives (Q1 and Q2) are shown below the spectrum.

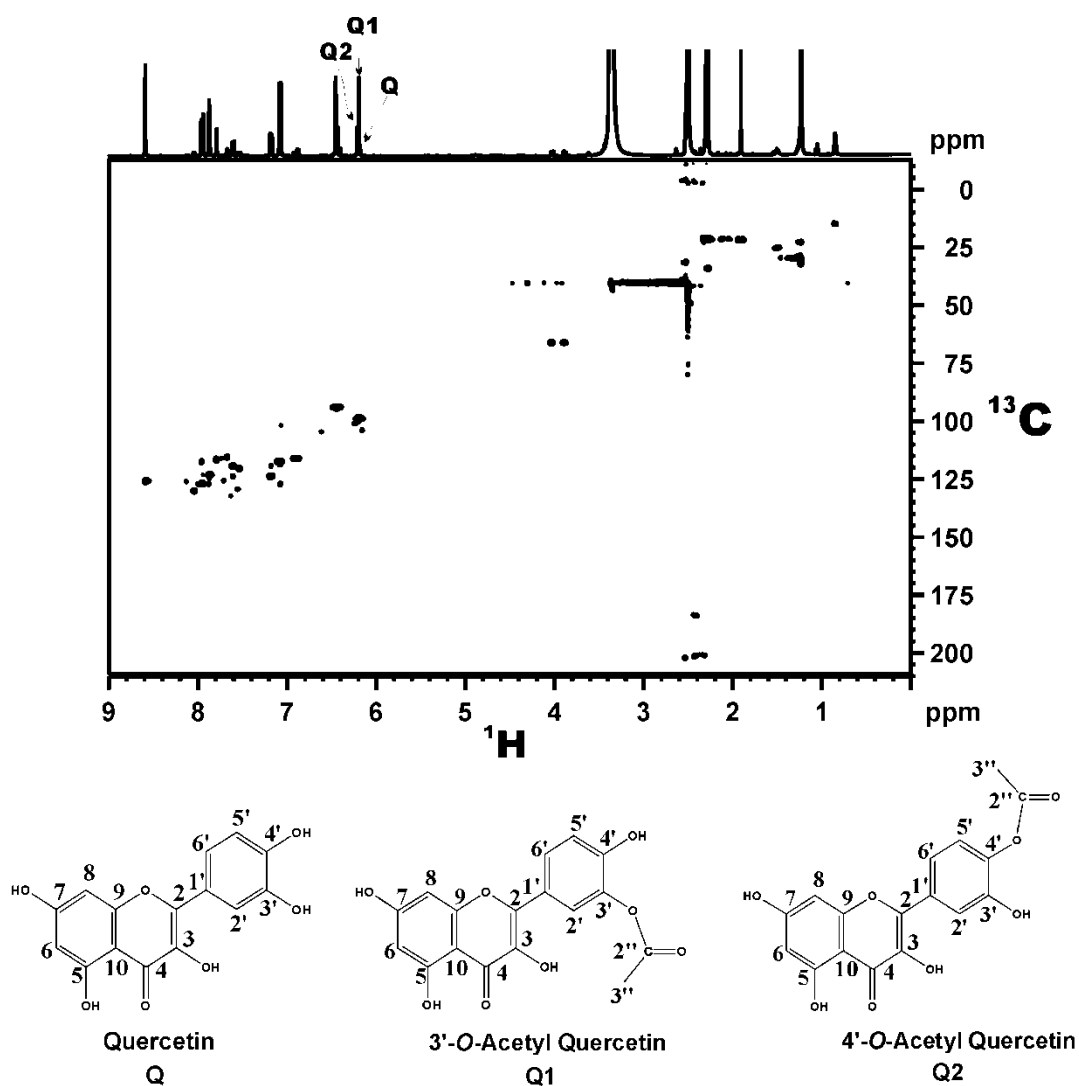


**Figure S10.** 500 MHz 2D  $^1\text{H}$ - $^{13}\text{C}$  HSQC NMR spectrum of quercetin derivatives Q1 and Q2 in 500  $\mu\text{l}$  DMSO- $d_6$  ( $T = 298$  K, number of scans = 25). Indicative resonances of the aromatic proton H6 of quercetin (Q) and its analogues (Q1 and Q2) are illustrated with arrows. The 2D structures of the two quercetin derivatives are shown below the spectrum.

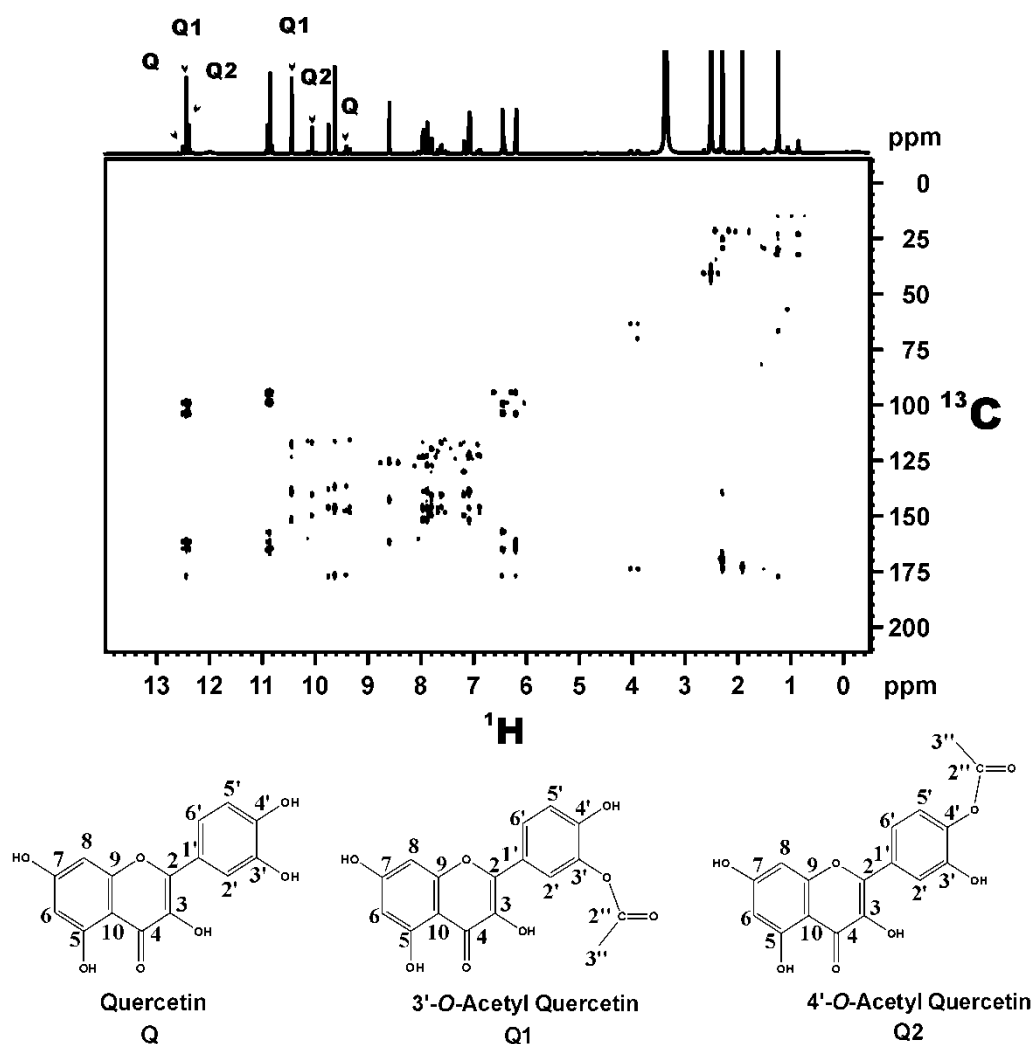


**Figure S11.** 500 MHz 2D  $^1\text{H}$ - $^{13}\text{C}$  HMBC NMR spectrum of quercetin derivatives Q1 and Q2 in 500  $\mu\text{l}$  DMSO- $d_6$  ( $T = 298$  K, number of scans = 76). Indicative resonances are illustrated for Q, Q1 and Q2 of proton OH5 (above 12 ppm), the OH4' of Q1 and OH3' Q2 as also the OH3' and OH4' of quercetin (Q). The 2D structures of the two quercetin derivatives are shown below.

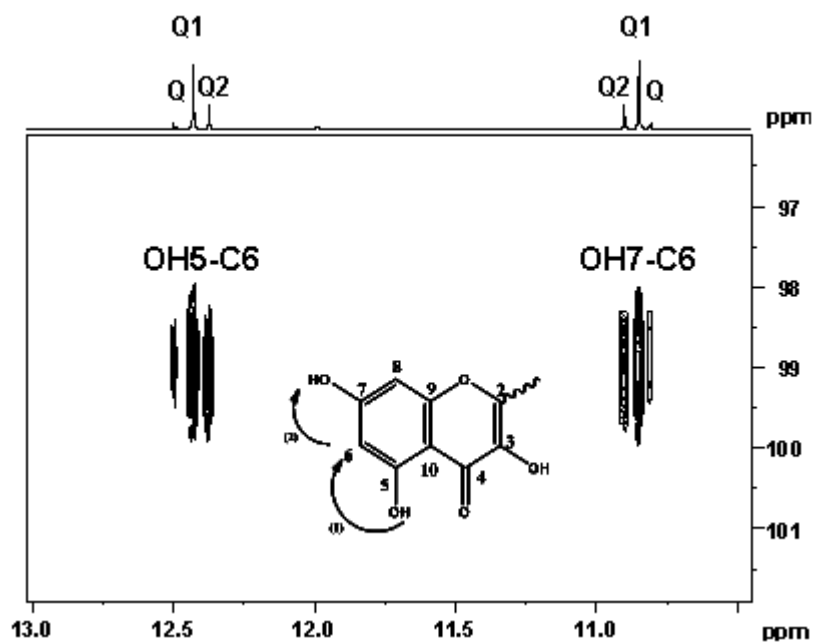


**Figure S12.** Selected region from a 500 MHz 2D  $^1\text{H}$ - $^{13}\text{C}$  HMBC NMR spectrum of the acylated derivatives of quercetin in 500  $\mu\text{l}$  DMSO- $d_6$  ( $T=298\text{ K}$ , number of scans = 76). The cross peaks of proton OH5 to carbon C(6) and the latter to proton OH7 of quercetin (Q) and its analogues (Q1 and Q2) are illustrated. These connectivities are also drawn as arrows in the relevant chemical substructure part.

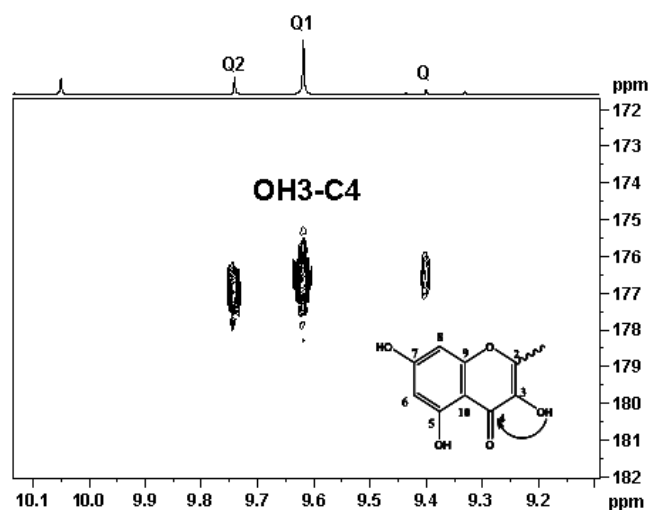


**Figure S13.** Selected region from a 500 MHz 2D  $^1\text{H}$ - $^{13}\text{C}$  HMBC NMR spectrum of the acylated derivatives of quercetin in 500  $\mu\text{l}$  DMSO- $d_6$  ( $T=298\text{ K}$ , number of scans = 76). The cross peak of proton OH3 to carbon C(4) of quercetin and its analogues are indicated.

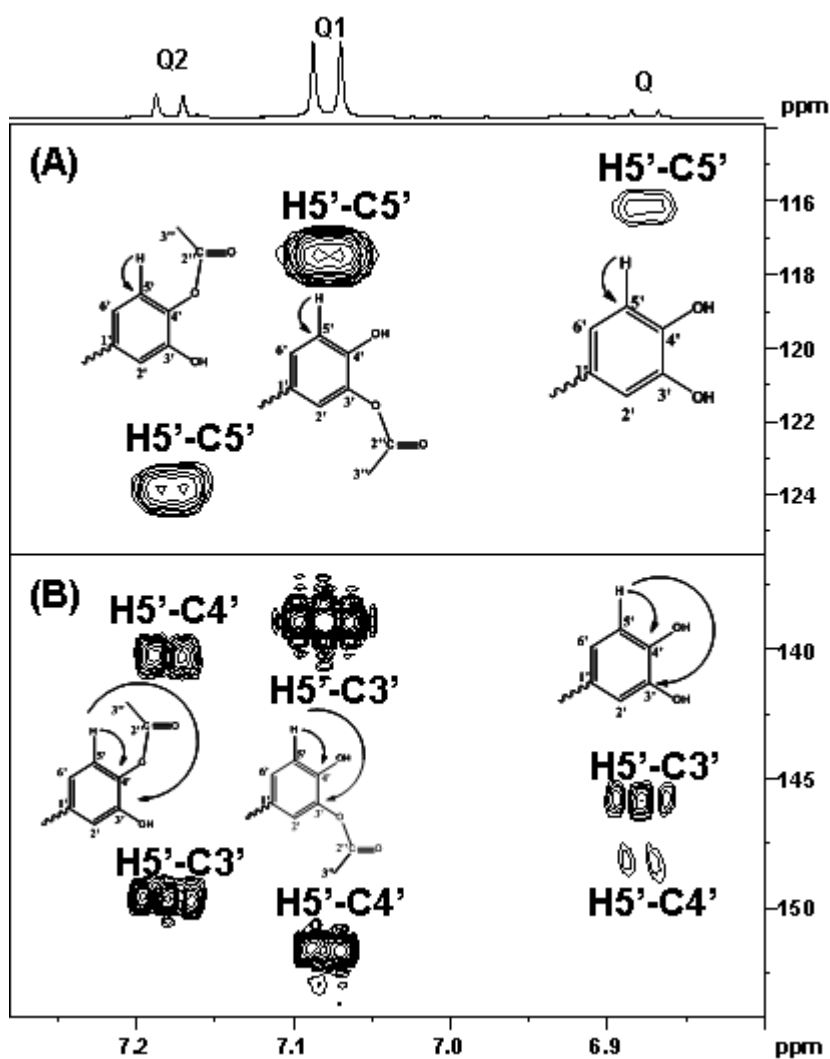


**Figure S14.** Selected region from a 500 MHz 2D  $^1\text{H}$ - $^{13}\text{C}$  HSQC spectrum (A) and 2D  $^1\text{H}$ - $^{13}\text{C}$  HMBC NMR spectrum (B) of the acylated derivatives of quercetin in 500  $\mu\text{l}$  DMSO- $d_6$  ( $T=298\text{ K}$ , number of scans = 76). The cross peak of aromatic proton H5' of B ring of flavonoids to carbons C(3') and C(4') of quercetin and its analogues are illustrated in panel (B).

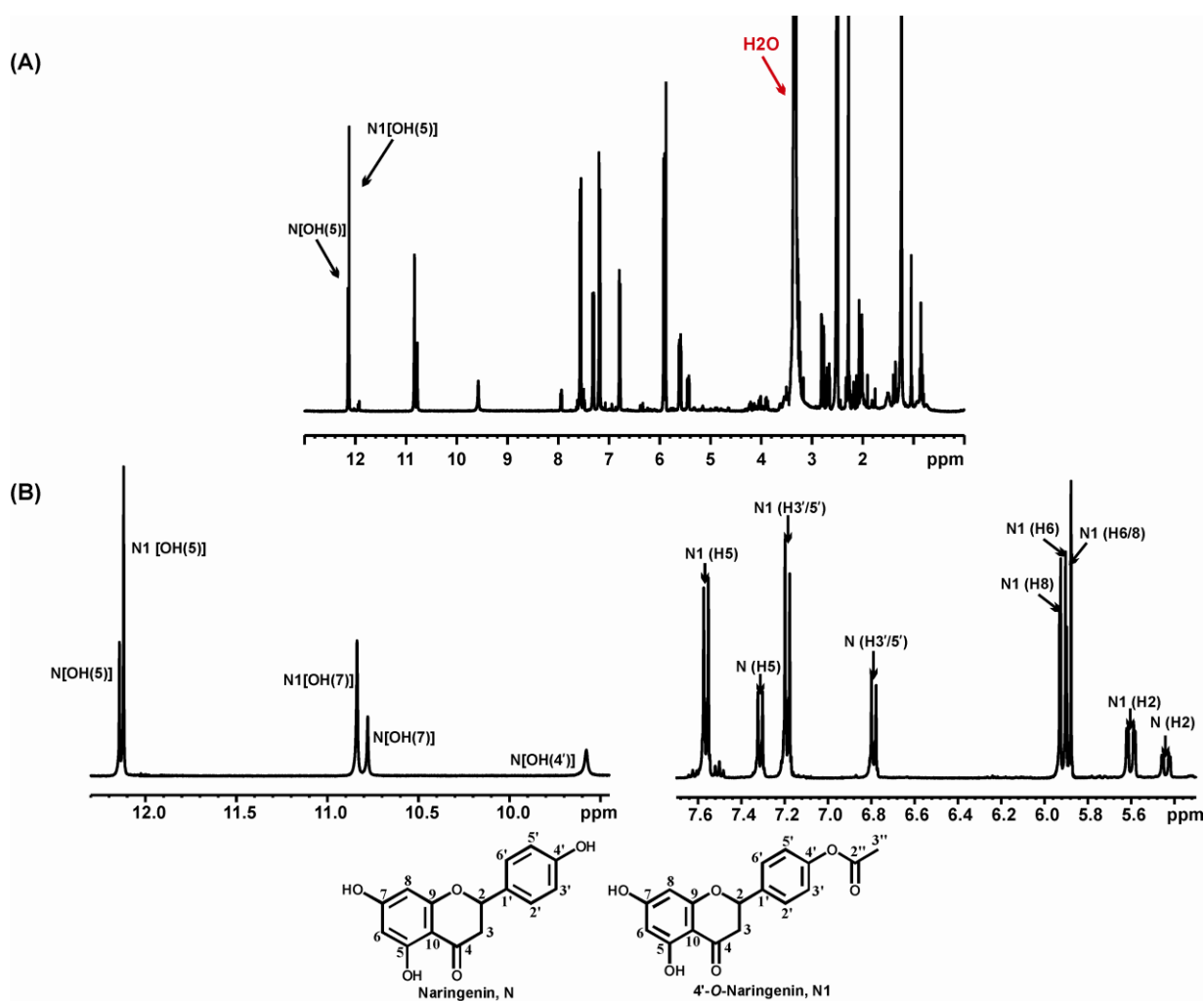


**Figure S15.** (A) 1D  $^1\text{H}$  NMR spectrum of naringenin (N) and its analogues (N1 and N2) in 500  $\mu\text{l}$  DMSO- $d_6$  ( $T = 298\text{ K}$ , number of scans = 256). (B) The left panel shows the  $-\text{OH}$  spectral region and the right one the aromatic spectral region. The two strongly deshielded resonances above 12.2 ppm correspond to the OH(5) protons of N and N1 participating in intramolecular hydrogen bonding with the carbonyl group CO(4). The assignment of selected absorptions for N and N1 are indicated in the relevant spectrum. The 2D structures of naringenin (N) and its derivative monoacylated (N1) are shown below the spectrum.

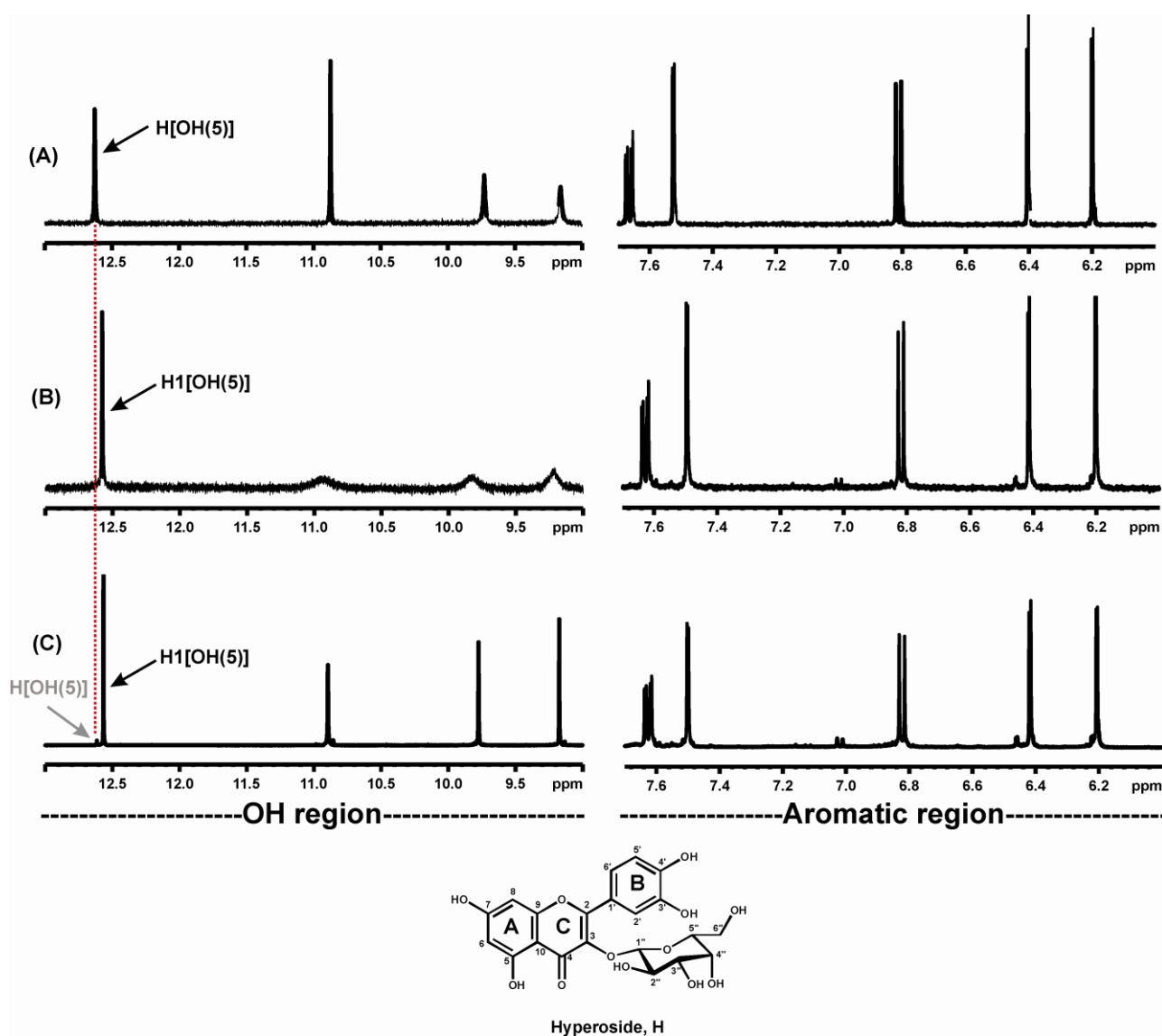


**Figure S16.** 500 MHz 1D  $^1\text{H}$  NMR spectrum of hyperoside (H) (2  $\mu\text{mol}$ ) and the enzymatically obtained acylation product (H1) in 400  $\mu\text{l}$  DMSO- $d_6$ . In (A) are illustrated the  $-\text{OH}$  and aromatic spectral regions of the authentic standard of the hyperoside and in (B) and (C) the relevant regions of the enzymatically retrieved reaction products before and after the addition of 44.50 nmol of picric acid (4.5  $\mu\text{l}$  from a 10.18 mM stock solution). The molar ratio of picric acid and acetyl hyperoside was 1:44. In (C) the two strongly deshielded resonances above 12.6 ppm correspond to the OH(5) protons of H (unreacted hyperoside) and H1 (acylated hyperoside) participating in intramolecular hydrogen bonding with the carbonyl group CO(4). The assignment of selected absorptions for H and H1 are indicated in the relevant spectrum. The 2D structure of hyperoside (H) is shown below the spectrum.

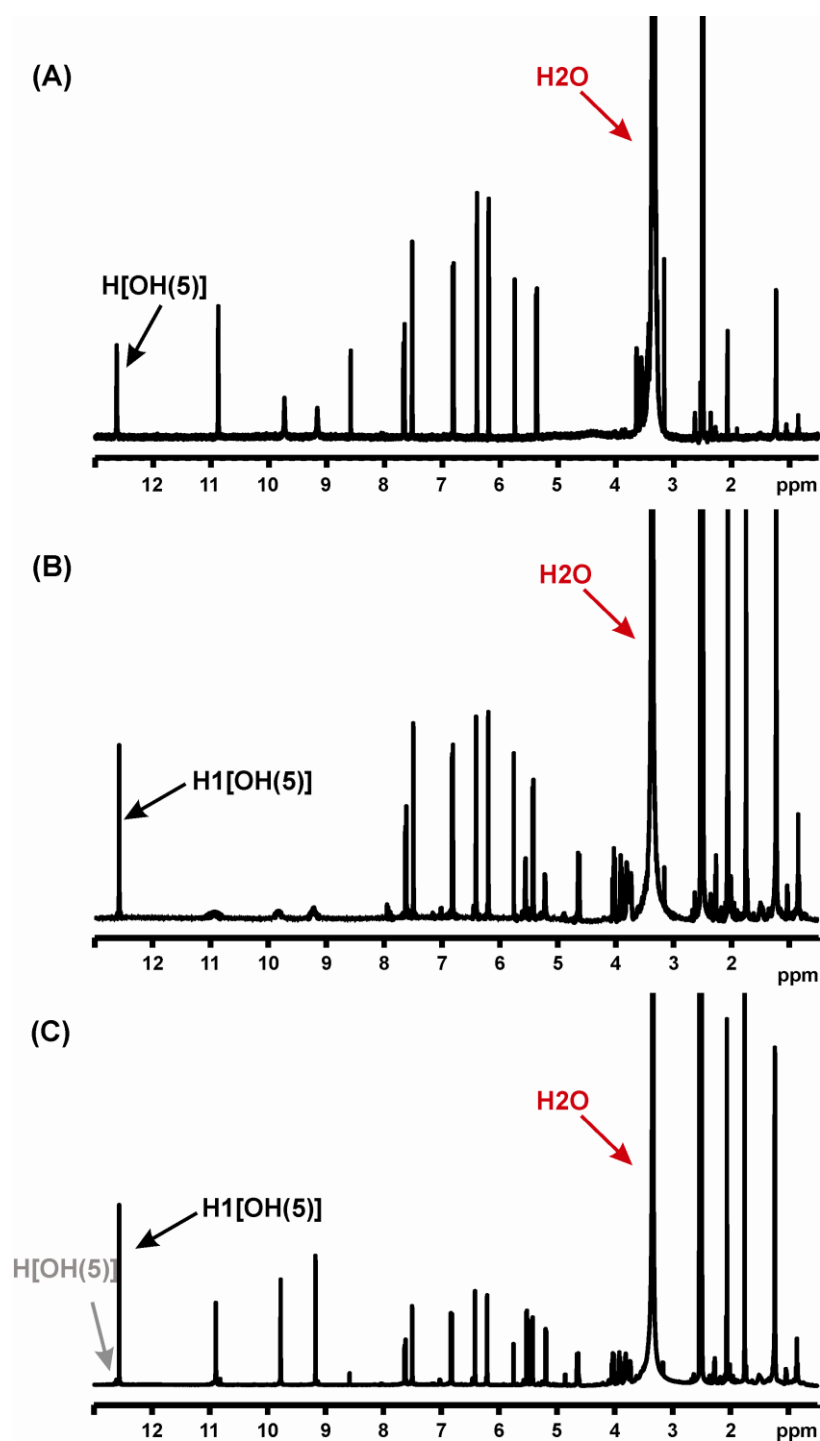


**Figure S17.** 500 MHz 1D <sup>1</sup>H NMR spectrum of hyperoside (H) (A) and the enzymatically obtained acylation product (H1) before (B) and after (C) the addition of 44.50 nmol of picric acid (4.5 μl from a 10.18 mM stock solution). The molar ratio of picric acid and acetyl hyperoside was 1:44. Samples were in 400 μl DMSO-d<sub>6</sub>.

**Table S1.**  $^1\text{H}$  and  $^{13}\text{C}$  chemical shift assignments of quercetin.

Quercetin		
Q		
	$^1\text{H}$	$^{13}\text{C}$
<b>2</b>		147.8
<b>3</b>	9.44 (1H, s)	136.8
<b>4</b>		176.9
<b>5</b>	12.54 (1H, s)	161.9
<b>6</b>	6.22 (1H, d, $J = 2.04$ )	98.8
<b>7</b>	10.85 (1H, s)	165.0
<b>8</b>	6.44 (1H, d, $J = 2.03$ )	94.0
<b>9</b>		157.4
<b>10</b>		103.9
<b>1'</b>		123.1
<b>2'</b>	7.71 (1H, d, $J = 2.18$ )	115.7
<b>3'</b>	9.37 (1H, s)	146.2
<b>4'</b>	9.66 (1H, s)	148.7
<b>5'</b>	6.92 (1H, d, $J = 8.47$ Hz)	116.2
<b>6'</b>	7.57 (1H, dd, $J = 2.23/ 6.28$ )	120.6

**Table S2.**  $^1\text{H}$  and  $^{13}\text{C}$  chemical shift assignments of the 3'-acetyl (Q1) derivative of quercetin. The assignment procedure followed for the determination of Q1 quercetin derivative can be seen in Figures S11 to S15.

	<b>3'-acetyl derivative</b>	
	<b>Q1</b>	
	$^1\text{H}$	$^{13}\text{C}$
<b>2</b>		146.7
<b>3</b>	9.66 (1H, s)	137.2
<b>4</b>		177.2
<b>5</b>	12.47 (1H, s)	161.9
<b>6</b>	6.23 (1H, d, $J = 2.03$ )	98.9
<b>7</b>	10.89 (1H, s)	165.2
<b>8</b>	6.50 (1H, d, $J = 2.03$ )	94.2
<b>9</b>		157.2
<b>10</b>		104.1
<b>1'</b>		123.2
<b>2'</b>	7.91 (1H, d, $J = 2.21$ )	123.3
<b>3'</b>		139.2
<b>4'</b>	10.48 (1H, s)	152.1
<b>5'</b>	7.12 (1H, d, $J$ $= 8.73$ Hz)	117.6
<b>6'</b>	7.99 (1H, dd, $J = 2.21/ 6.44$ )	127.2
<b>COMe</b>		169.9
<b>COMe</b>	2.33 (3H, s)	21.4

**Table S3.**  $^1\text{H}$  and  $^{13}\text{C}$  chemical shift assignments of the 4'-acetyl (Q2) derivative of quercetin. The assignment procedure followed for the determination of the Q2 quercetin derivative can be seen in Figures S11 to S15.

	4'-acetyl derivative	
	Q2	
	$^1\text{H}$	$^{13}\text{C}$
<b>2</b>		146.4
<b>3</b>	9.78 (1H, s)	138.2
<b>4</b>		177.4
<b>5</b>	12.41 (1H, s)	161.9
<b>6</b>	6.25 (1H, d, $J = 2.03$ )	98.9
<b>7</b>	10.94 (1H, s)	165.4
<b>8</b>	6.47 (1H, d, $J = 2.03$ )	94.1
<b>9</b>		157.4
<b>10</b>		104.2
<b>1'</b>		130.3
<b>2'</b>	7.83 (1H, d, $J = 2.12$ )	116.7
<b>3'</b>	10.09 (1H, s)	150.0
<b>4'</b>		140.6
<b>5'</b>	7.22 (1H, d, $J = 8.50$ Hz)	124.0
<b>6'</b>	7.64 (1H, dd, $J = 2.12/ 6.37$ )	119.4
<b>COMe</b>		169.8
<b>COMe</b>	2.32 (3H, s)	21.3

**Table S4.**  $^1\text{H}$  and  $^{13}\text{C}$  chemical shift assignments of Naringenin.

	<b>Naringenin</b>	
	<b>N</b>	
	$^1\text{H}$	$^{13}\text{C}$
<b>2</b>	5.44	78.9
<b>3 cis</b>	2.67	42.48
<b>3 trans</b>	3.25	42.48
<b>4</b>	-	196.91
<b>5</b>	12.14	164.2
<b>6</b>	5.88	96.6
<b>7</b>	10.78	167.3
<b>8</b>	5.88	95.5
<b>9</b>	-	163.2
<b>10</b>	-	102.6
<b>1'</b>	-	
<b>2'</b>	7.31	129.2
<b>3'</b>	6.79	115.9
<b>4'</b>	9.58	158.6
<b>5'</b>	6.79	115.9
<b>6'</b>	7.31	129.2

**Table S5.**  $^1\text{H}$  and  $^{13}\text{C}$  chemical shift assignments of the 4'-acetyl (N1) derivative of naringenin.

	<b>4'-acetyl derivative</b>	
	<b>N1</b>	
	$^1\text{H}$	$^{13}\text{C}$
<b>2</b>	5.60	78.2
<b>3 cis</b>	2.80	42.6
<b>3 trans</b>	3.29	42.6
<b>4</b>	-	196.91
<b>5</b>	12.12	164.2
<b>6</b>	5.90	96.6
<b>7</b>	12.84	167.3
<b>8</b>	5.93	95.9
<b>9</b>	-	163.4
<b>10</b>	-	102.6
<b>1'</b>	-	136.3
<b>2'</b>	7.56	128.4
<b>3'</b>	7.19	122.3
<b>4'</b>	-	150.9
<b>5'</b>	7.19	122.3
<b>6'</b>	7.56	128.4
<b>COMe</b>	-	169.8
<b>COMe</b>	2.28	21.93